Theoretical Study of the CO$_2$ Adsorption by Zeolitic Imidazolate Frameworks (ZIFs)

Journal:	*The Journal of Physical Chemistry*
Manuscript ID	jp-2017-04977t.R2
Manuscript Type:	Article
Date Submitted by the Author:	26-Aug-2017
Complete List of Authors:	Izzaouihda, Safia; Facu, CHIMIE Abou El Makarim, Hassna; University Mohammed V, Faculty of Sciences Benoit, David; University of Hull, Chemistry Komiha, Najia; University Mohammed V, Faculty of Sciences

SCHOLARONE™
Manuscripts

Theoretical Study of the CO$_2$ Adsorption by Zeolitic Imidazolate Frameworks (ZIFs)

Safia IZZAOUIHDA[1*], Hassna ABOU El MAKARIM[1], David M. BENOIT[2], Najia KOMIHA[1*]

[1]Laboratory LS3ME, Team Theoretical Chemistry and Molecular Modeling, University of Mohammed V Faculty of Sciences, Department of Chemistry, BP1014 Rabat Morocco
[2]E.A. Milne Centre for Astrophysics & G.W. Gray Centre for Advanced Materials, Chemistry, School of Mathematical and Physical Sciences, University of Hull, Hull, HU6 7RX, UK

*Corresponding authors: komiha@fsr.ac.ma; safiafssm@gmail.com

Abstract

Density functional theory with Grimme's empirical correction, DFT-D3, has been used to examine the adsorption of a carbon dioxide molecule by different sets of zeolitic imidazolate framework materials (ZIF-1 to -4, -6 to -10, and -zni). We have calculated the interaction energy, the dipole moment variation, and the charge density difference for the different CO$_2$@ZIF structures. Our study shows a strong relationship between the CO$_2$ adsorption energy and the volume of the cavities of the ZIFs: the capture of carbon dioxide depends on the shape and size of the ZIFs pore in which CO$_2$ has been inserted. The physisorption phenomena that govern the adsorption of CO$_2$ molecule require both π-stacking interactions and hydrogen-like bonding. We have found that adsorption does not change the geometry of CO$_2$, but it induces a significant structural change in some ZIF structures.

1. Introduction

The increasing concentration of CO$_2$ gas in the atmosphere is one of the major concerns of the scientific community today. Numerous studies have begun to explore this topic and propose solutions to reduce the high concentration of this greenhouse gas.

Using copolymerization of either Zn(II) or Co(II) ions with imidazolate-type linkers (Im), Yaghi and his co-workers have pioneered the synthesis of new materials which possess both a high porosity and an excellent chemical stability: the zeolitic imidazolate frameworks (ZIFs) [1]. These new classes of porous crystals are named so due to their structural proximity to zeolites. The equilibrium value of the angle M-Im-M in ZIFs (where M stands for Zn or Co cations and Im stands for the imidazolate linker) is 145 ° which is equal to the Si-O-Si angle in zeolites [2]. The development and recent progress of different synthesis strategies to generate ZIF materials have been analyzed and summarized by Chen et al [3].

Zeolitic imidazolate frameworks have an exceptional ability to capture and separate CO_2 from a gas mixture. A series of ZIFs have been recently examined for their potential to separate CO_2 from CH_4, CO, O_2 and N_2 gases [4,5]. The nature of the interaction between CO_2 and ZIFs has been the subject of numerous theoretical studies [6–9]. Understanding the physical phenomena governing this interaction is of academic as well as industrial importance. Different studies have approached this issue by investigating the interaction of CO_2 with ZIF organic units. The interactions between imidazole and CO_2 molecules are mainly dominated by Van der Waals forces, including induction, dispersion and electrostatic effects [10]. Moreover, the proposed $CO_2@[Zn^{q+}Im]$ (where q = 0,1, 2; Im = imidazole) models of the interactions of CO_2 with these subunits of zeolitic imidazolate frameworks show that CO_2 molecules can be adsorbed through π-stacking as well as σ-type hydrogen-bonding interactions [11]. The aim of the present work is to study the physisorption properties of CO_2 with a set of ZIF materials. We have limited this work to compounds with chemical composition $Zn(Im)_2$.

This paper is structured as follows: Section 2 describes the details of the computational approach used to generate our results. In section 3, we present the optimized set of ZIFs structures (section 3.1) which are used as a starting point to trapping a single CO_2 molecule. In section 3.2 we report our DFT and DFT-D3 calculations for adsorbed CO_2 molecules in the cavities of the ZIF. The analysis of the charge density transformation in $CO_2@ZIFs$ complexes are reported in subsection 3.3. The last section is reserved to our conclusions.

2. Computational methods

In this study, we have adopted periodical calculations using the QUICKSTEP module [12] built in the CP2K program [13] which allows DFT calculations [14,15]. This module uses the GPW method [16] allowing a better treatment of the electrostatic interactions. The GGA functional PBE [17] has been used to describe exchange-correlation effects.

We consider ZIF structures that have been synthesized as crystals by copolymerization of Zn(II) with imidazolate-type linkers by Yaghi and his co-workers [1]: ZIF-1, -2, -3, -4, -6 and 10, and the one (zni) synthesized by Lehnert and Seel [18]. Moreover, we also investigate the theoretical imidazolate $Zn(Im)_2$ models, ZIF-7, ZIF-8 and ZIF-9 obtained by Lewis et al. [19] by the removal of substituents from the imidazolate rings (-CH3, $-C_6H_4$). The ZIF details have been extracted from the crystallographic data base CCDC [20], eliminating extra-framework species and the imidazolate substituents when required.

To improve the description of the long-range dispersion interactions, we have used the DFT-D3 method where DFT is corrected using an empirical Van der Waals correction suggested by Grimme et al. [21]. For each atom we have used the TZV2P MOLOPT-GTH basis set [22] except for Zn atoms for which we have used a DZVP MOLOPT-GTH basis[22]. The GTH pseudopotentials in our calculations have been generated from fully relativistic all-electrons calculations for each atom[23–25].

Furthermore, to minimize the total ground state energy, we have used the orbital transformation method (OT) [26], where all calculations have been performed at the Γ–point of the Brillouin zone. Periodic boundary conditions have been applied in xyz directions. The BFGS optimization method has been used for all the calculations using default convergence criteria and default energy SCF convergence criterion of 10^{-5} Hartree.

3. Results and discussion

1. Geometry optimization of ZIF structures

In the first stage, we have performed a geometry optimization to determine the equilibrium structures for the different ZIFs (ZIF-1 to -4, -6 to 10, and zni). The total energy has been calculated using both DFT/PBE and PBE-D3 methods, the latter leading to an improvement of the long-range dispersion interactions. Table 1 summarizes the calculations results along with volume and framework density.

ZIFs	Composition	CCDC Code	Number of Zn atoms per unit	Volume in Å³	Framework density (Zn/Volume) in nm⁻³	E_{ZIFs} in eV/Zn	
						DFT/PBE	DFT/PBE-D3
1	$Zn(Im)_2$	VEJYEP	8	2310.2 [a]	3.46 [a]	−3757.010	−3757.660
				2195.8 [b]	3.64 [b]		
2	$Zn(Im)_2$	VEJYIT	16	5691.6 [a]	2.81 [a]	−3756.990	−3757.561
				5706.6 [b]	2.80 [b]		
3	$Zn(Im)_2$	VEJYOZ	16	6031.4 [a]	2.65 [a]	−3757.009	−3757.579
				6024.1 [b]	2.66 [b]		
4	$Zn(Im)_2$	VEJYUF	16	4380.5 [a]	3.65 [a]	−3757.014	−3757.680
				4344.9 [b]	3.68 [b]		
6	$Zn(Im)_2$	EQOCOC	8	3594.3 [a]	2.22 [a]	−3757.019	−3757.560
				3470.0 [b]	2.31 [b]		
7*	$Zn(Im)_2$	–	6	2427.1 [a]	2.47 [a]	−3756.973	−3757.530
				2404.8 [b]	2.50 [b]		
8*	$Zn(Im)_2$	–	6	2474.7 [a]	2.42 [a]	−3757.021	−3757.589
				2452.6 [b]	2.47 [b]		
9*	$Zn(Im)_2$	–	18	7223.9 [a]	2.49 [a]	−3756.973	−3757.533
				7178.9 [b]	2.51 [b]		
10	$Zn(Im)_2$	VEJZIU	16	7312.7 [a]	2.19 [a]	−3757.024	−3757.572
				7105.4 [b]	2.25 [b]		
zni	$Zn(Im)_2$	IMIDZB	16	3611.7 [a]	4.43 [a]	−3757.034	−3757.822
				3440.7 [b]	4.66 [b]		

Table 1: Optimized geometry and experimentally determined parameters ([b]) of ZIFs (PhIm = benzimidazolate, mIm = methylimidazole); simulated with the $Zn(Im)_2$ composition. (*) and ([a]) refer to the model structures proposed by Lewis et al. [19]. The table shows the chemical composition, the

CCDC codes, the number of Zn atom per unit, the unit volume, the framework density (expressed as the number of Zn atoms per volume unit) and the total energies of different ZIF structures.

In Figure 1 we have plotted the calculated total energies of our ZIF structures as a function of their framework densities. The total energy of the most stable structure, zni, is taken as a reference point for the other energies.
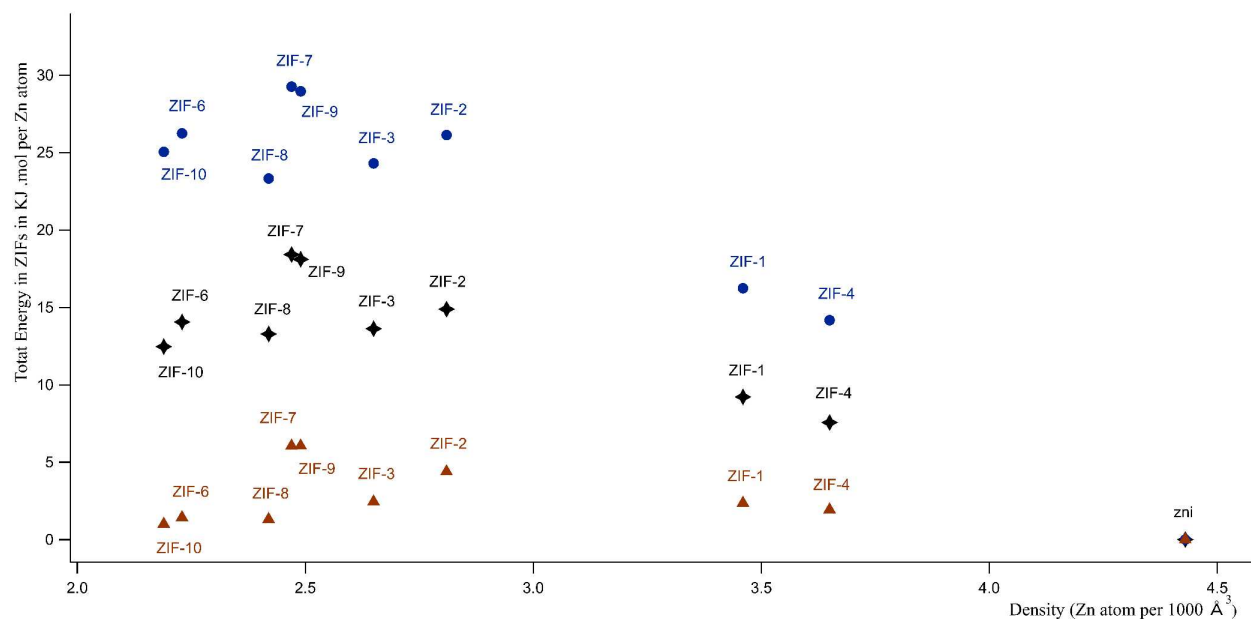

Figure 1: Variation of total energy of the ZIF using DFT method versus their framework density. zni energy taken as reference. (♦) Energy calculated by Lewis et al. [19]. The red triangles and the blue circles are our calculated PBE and PBE-D3 energy respectively.

It should be emphasized that the trend of the variation of our ZIFs energy calculated in terms of their framework densities is in excellent agreement with the one obtained by Lewis et al. [19]. We note that the synthesized ZIFs (ZIF-1 to ZIF-6, ZIF-10 and zni) present the most stable structures. For this set of materials, it is noticed that as the density increases, the ZIFs structures show generally more stability. The modified ZIF-7 and ZIF-9 are the less stable structures, probably due to the fact that there are no substituents in the imidazolate rings that can increase the number of possible hydrogen bonds and consolidate the ZIF. We observe that pure PBE systematically under-estimates the relative ZIF energy, compared to the results of Lewis et al. [19], but that conversely PBE-D3 tends to over-estimate the same relative energies. This highlights both the influence and subtle balance of dispersion interactions in ZIF structures.

2. Carbon dioxide adsorption

We have trapped one CO_2 molecule in the center of the cavity of each optimized ZIF structures obtained earlier in order to study their ability to adsorb one CO_2 molecule. The shape of the cavity and the pore size can differ from one ZIF to the other (i. e. the cavity of ZIF-8 contains 8 Zn atoms and 4 Zn atoms in ZIF-1). We will see later how this influences the interaction energy of CO_2 in the different ZIF structures.

We have performed a full geometry optimization with fixed cell parameters for each CO_2@ZIF complex. The complexes obtained are shown in Figure 2.
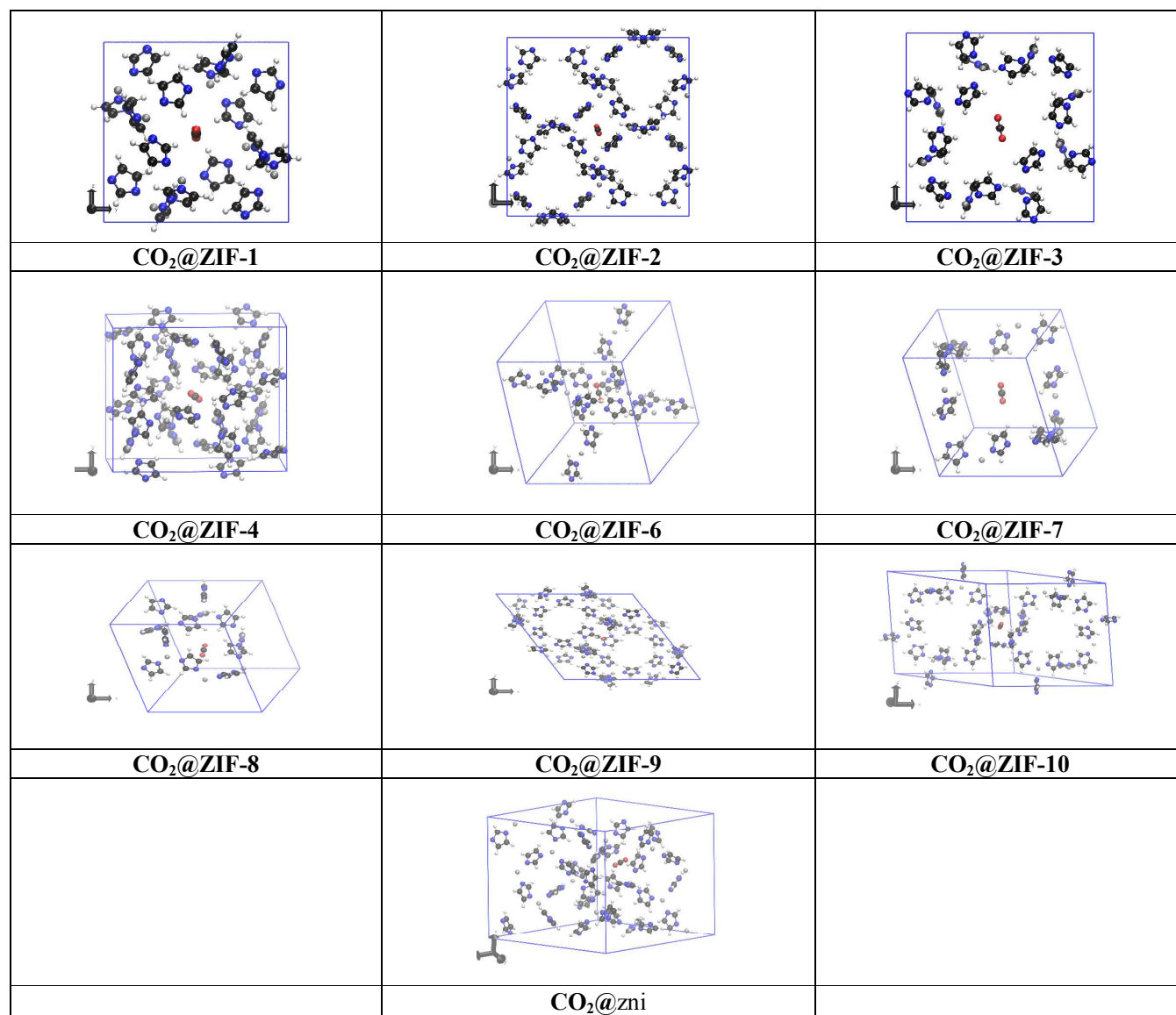

CO_2@ZIF-1	**CO_2@ZIF-2**	**CO_2@ZIF-3**
CO_2@ZIF-4	**CO_2@ZIF-6**	**CO_2@ZIF-7**
CO_2@ZIF-8	**CO_2@ZIF-9**	**CO_2@ZIF-10**
	CO_2@zni	

Figure 2: Optimized geometries of the different CO_2@ZIFs complexes where the CO_2 molecule is trapped in the cavity center of each ZIF structures.

We noticed that no geometrical distortion of the carbon dioxide molecule occurs, in the cavity center of the ZIF structures. The CO_2 molecule stays linear with equal CO bond lengths. The bond length of CO_2 is found to be 1.17 Å in all different sets of ZIF which it is in good agreement with the experimental value (1.16 Å) for the isolated molecule [27]. However, the trapped CO_2 molecule induces a structural distortion on most of the ZIF molecules; the imidazolate rings reorient itself towards the CO_2 molecule. Moreover, in

most of the CO_2@ZIF complexes, we observe a small variation of the Zn–Zn distances (0.01 Å) with respect to the starting values.

We also characterize the interactions between CO_2 and ZIF materials by means of the variation of the dipole moments before and after complexation (see Table 2). In most cases, ZIF-1, -2, -4, -6, -7, -9 and -10, the ZIF structures are initially apolar, the dipole moment calculated is nearly zero. ZIF-3 and -8 are weakly polar and the most stable structure, zni shows the largest dipole moment (1.73 Debye). After the complexation, the dipole moments vary slightly as reported in Table 2.

ZIFs	Number of Zn atoms in ZIFs cavity	Dipole moments in Debye	
		Clean structure	Complexed structure
1	8	0.00	0.02
2	4	0.00	0.30
3	16	0.23	0.21
4	8	0.00	0.07
6	4	0.00	0.09
7*	6	0.00	0.01
8*	6	0.11	0.43
9*	4	0.00	0.02
10	4	0.01	0.35
Zni	4	1.73	1.71

Table 2: Calculated dipole moments for the different ZIF structures before and after the complexation with the CO_2 molecule.

Using the DFT-D3/PBE method, we have calculated the interaction energy between the CO_2 molecule and the ZIF ($E_{int}(CO_2$@ZIF)) according to the following formula:

$$E_{int}(CO_2@ZIF) = E_{opt}(CO_2@ZIF) - [E_{opt}(ZIF) + E_{opt}(CO_2)]$$

where $E_{opt}(CO_2$@ZIF), $E_{opt}(CO_2)$ and $E_{opt}(ZIF)$ are the total energies of the optimized geometries of the complex CO_2@ZIF, the isolated CO_2, and the isolated ZIF respectively. Our results are shown in Table 3, along with computed atomic charges and charge transfer estimation using Mulliken population analysis[28].

1
2
3
4
5
6
7
8
9
10
11
12
13
14
15
16
17
18
19
20
21
22
23
24
25
26
27
28
29
30
31
32
33
34
35
36
37
38
39
40
41
42
43
44
45
46
47
48
49
50
51
52
53
54
55
56
57
58
59
60

ZIF	Net atomic charge (e) of CO_2			Charge transfer (e) between CO_2 and different ZIFs	E_{int} $(CO_{2@}ZIFs)$ in kJ mol^{-1}
	C	O	O		
1	**0.29011**	**−0.13910**	**−0.14468**	0.00632	−17.31
	0.30781	−0.15393	−0.15389		
2	**0.29556**	**−0.12740**	**−0.17541**	0.00726	−10.14
	0.31022	−0.15511	−0.15511		
3	**0.30343**	**−0.15161**	**−0.15292**	−0.00110	−6.71
	0.31154	−0.15572	−0.15582		
4	**0.33953**	**−0.17462**	**−0.17070**	−0.00579	−25.00
	0.31030	−0.15515	−0.15515		
6	**0.29375**	**−0.15030**	**−0.15535**	−0.01190	2.31
	0.31020	−0.15510	−0.15510		
7	**0.31138**	**−0.15438**	**−0.15683**	0.00017	−3.28
	0.31041	−0.15517	−0.15524		
8	**0.33529**	**−0.16983**	**−0.17137**	−0.00593	−19.70
	0.31133	−0.15566	−0.15567		
9	**0.30744**	**−0.16094**	**−0.15521**	−0.00871	−16.13
	0.31020	−0.15509	−0.15511		
10	**0.29409**	**−0.12418**	**−0.17825**	−0.00834	−17.82
	0.31007	−0.15502	−0.15505		
zni	**0.29421**	**−0.14824**	**−0.13758**	0.00839	−27.71
	0.31011	−0.15509	−0.15502		

Table 3: Calculated energies and charge transfer ($\Delta\rho$) between CO_2 and the different ZIFs materials calculated as: $\Delta q = q(CO_2)_{ZIF} − q(CO_2)_{free}$ where $q(CO_2)_{ZIF}$ is the CO_2 charge molecule in ZIF material (in bold letters) and $q(CO_2)_{free}$ is the charge of CO_2 free molecule (normal letters).

All the results show a weak charge transfer between CO_2 and ZIFs indicating that we have a physisorption process. The data in the Table 3 shows that the interaction energy between CO_2 and the ZIFs in the cavity center is mainly dominated by Van der Waals forces. In general, we can conclude that as the ZIF cavity diameter decreases, the number of imidazolates linkers surrounding the CO_2 molecule increases and the interaction energy of $CO_2@ZIFs$ increases. This is the case for CO_2 in a zni cavity. However, for ZIF-6 with a small central cavity, the $CO_2@ZIF-6$ complex has a positive value of the interaction energy. This shows the absence of a tendency to fix CO_2 despite a favorable charge transfer. For ZIF-3 and ZIF-7 the interaction energy is weak since these two materials have the largest cavity compared to the others (d_{ZIF-3} = 8.02 Å, d_{ZIF-7} = 4.31 Å; d is the diameter of the largest sphere that will fit into the framework [1]). Also, the insertion of CO_2 in these two cavities does not affect their geometries, this is confirmed by the low variation of their dipole moment (~0.01Debye).

To quantify the correlation between structural parameters and the interaction energy, we plotted the variation of the interaction energy of CO_2@ZIF complexes as a function of the ZIF framework densities expressed as the number of Zn sites per ZIF unit volumes (Figure 3).
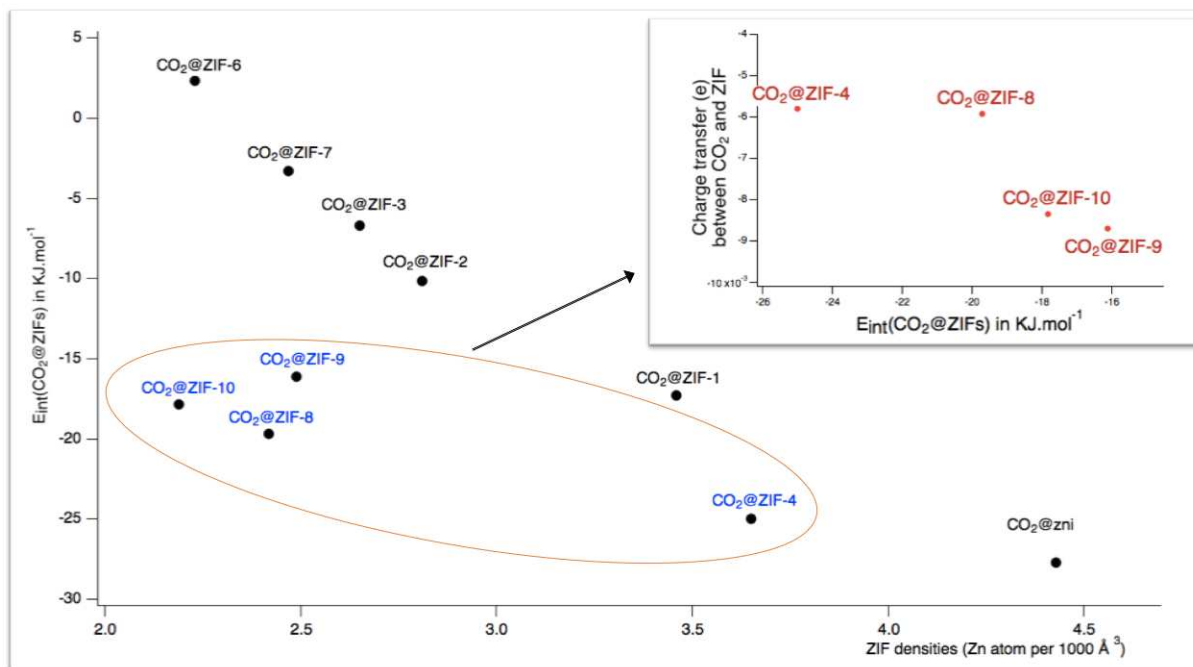

Figure 3: variation of CO_2@ZIF interaction energy as a function of ZIF framework densities expressed as the number of Zn sites per ZIF unit volumes. In the upper panel is and the charge transfer between CO_2 and ZIF as a function of CO_2@ZIF interaction energy.

It appears that two distinct groups can be identified among the known CO_2@ZIF complexes structures: a first group consisting of CO_2@ZIF-1, -2, -3, -6, -7, and zni where the CO_2@ZIF interaction energy and the ZIFs density framework varied concomitantly, and second group consisting of CO_2@ZIF-4, -8, -9, and -10, the most interacting complexes. For this last group, we looked to the variation of charge transfer between CO_2 and the ZIF structures as a function of interacting CO_2@ZIFs energy. We find that the charge transfers increase as the CO_2@ZIFs interaction energy increases.

Indeed, in ZIFs structures, the organic frameworks are linked to metal ions through nitrogen atoms which are the most active sites of the imidazolate ligands. In the presence of CO_2, the attachment occurs through NNCH—OCO or CH–CH—OCO hydrogen-like bonds or through π-staking interactions depending on the orientation of the imidazolate linkers in the ZIF cavity. More details are provided in the next section.

3. The charge transfer analysis

The process of CO_2 adsorption by zeolitical imidazolate frameworks occurs through a physisorption interaction. In order to understand the nature of the binding process, we have calculated the charge density difference $\Delta\rho$ for the different CO_2@ZIF complexes using the following formula:

$$\Delta\rho = \rho(CO_2@ZIFs) - \rho(CO_2) - \rho(ZIF)$$

where $\rho(CO_2@ZIFs)$ is the charge density of the $CO_2@ZIF$ complex; $\rho(CO_2)$ and $\rho(ZIF)$ are the charge densities of the non-interacting CO_2 and ZIF molecules respectively at the geometry of the complex.

Our computed charge densities differences are plotted in Figure 3 to allow for a better understanding of the $CO_2@ZIF$ interactions and explain the variations of the interaction energies calculated for the different $CO_2@ZIF$ complexes. Two interaction cases occur: low charge density transfer for $CO_2@ZIF-3$ and $CO_2@ZIF-7$ and strong interaction for the rest of the $CO_2@ZIFs$ complexes.
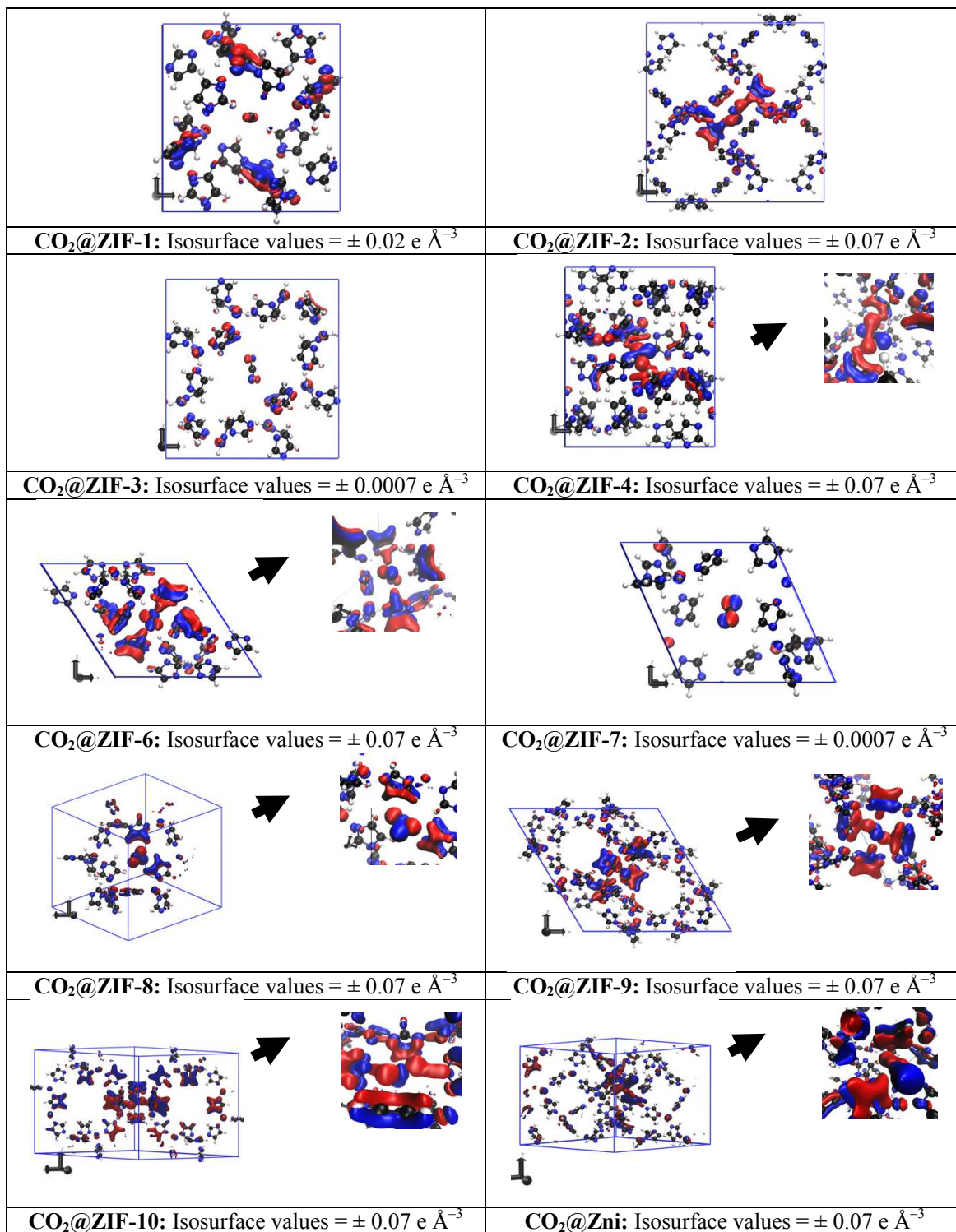
Figure 4: Charge density calculated for different CO_2@ZIF complexes. Regions of accumulation/depletion are marked in blue/red, respectively.

In figure 4 we used different iso-charge surfaces to better display the computed charge density transfer. The classification of the interaction energies is shown in Table 3. Interestingly, the charge density

transfer between CO_2 and ZIF-9 shows that CO_2 is fixed trough π-staking interactions with the two close imidazolates. For $CO_2@ZIF$-10 the interaction originates from the formation of two hydrogen bonds.

4. Conclusion

In the present work, we carried out a comparative study of the adsorption of a CO_2 molecule by different zeolitic imidazolate framework materials. This study examines two types of structures: the synthesized one (ZIF-1 to -4, -6, -10 [1] and zni [18]) and the proposed models by Lewis (ZIF-7 to -9 [19]). The common point is that they have all the same chemical composition $Zn(Im)_2$. Using DFT/PBE and DFT-D3/PBE calculations, we have shown that the capture of the carbon dioxide depends on the nature of the dimension of the cavity in which it is inserted; as it increases, the interaction energy of $CO_2@ZIF$ decreases. We have also validated the two proposed ZIF structures ZIF-8 and ZIF-9 for CO_2 capture.

The capture of CO_2 is due to physisorption phenomena. To understand the nature of the interactions of CO_2 in the ZIFs cavity, we have calculated the charge density which recalls the formation of two type of CO_2 attachment: π-stacking and hydrogen-like bond.

We have shown that the insertion of a CO_2 molecule in the different ZIF cavities induces a rearrangement of the imidazolate linkers and a slight variation of the dipole moments for the different ZIF structures is observed. The capture of CO_2 occurs without any structural distortion for the guest molecule. This allows us to start thinking about how to make this molecule more active.

The simple model proposed in this work using single CO_2 molecule in the center of the ZIF cavities to describe CO_2 capture by zeolitic imidazolate frameworks may not be sufficient to describe all CO_2–ZIF interactions. In addition, the presence of several CO_2 molecules requires to also consider the CO_2–CO_2 interactions[29], this could be the subject of a future work in this field.
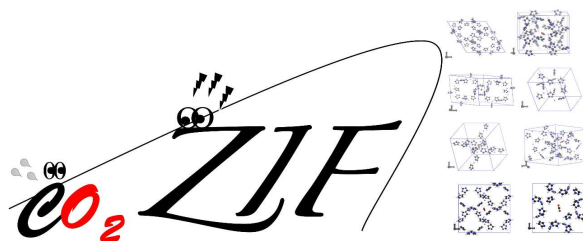
Acknowledgements

References

(1)   Park, K. S.; Ni, Z.; Côté, A. P.; Choi, J. Y.; Huang, R.; Uribe-Romo, F. J.; Chae, H. K.; O'Keeffe, M.; Yaghi, O. M. Exceptional Chemical and Thermal Stability of Zeolitic Imidazolate Frameworks. *Proc. Natl. Acad. Sci.* **2006**, *103* (27), 10186–10191.

(2)   Li, Y.; Yu, J. New Stories of Zeolite Structures: Their Descriptions, Determinations, Predictions, and Evaluations. *Chem. Rev.* **2014**, *114* (14), 7268–7316.

(3)   Chen, B.; Yang, Z.; Zhu, Y.; Xia, Y. Zeolitic Imidazolate Framework Materials: Recent Progress in Synthesis and Applications. *J. Mater. Chem. A* **2014**, *2* (40), 16811–16831.

(4)   Wang, B.; Côté, A. P.; Furukawa, H.; O'Keeffe, M.; Yaghi, O. M. Colossal Cages in Zeolitic Imidazolate Frameworks as Selective Carbon Dioxide Reservoirs. *Nature* **2008**, *453* (7192), 207–211.

(5)   Banerjee, R.; Furukawa, H.; Britt, D.; Knobler, C.; O'Keeffe, M.; Yaghi, O. M. Control of Pore Size and Functionality in Isoreticular Zeolitic Imidazolate Frameworks and Their Carbon Dioxide Selective Capture Properties. *J. Am. Chem. Soc.* **2009**, *131* (11), 3875–3877.

(6)   McDaniel, J. G.; Yu, K.; Schmidt, J. R. Ab Initio, Physically Motivated Force Fields for CO2 Adsorption in Zeolitic Imidazolate Frameworks. *J. Phys. Chem. C* **2012**, *116* (2), 1892–1903.

(7)   Liu, J.; Keskin, S.; Sholl, D. S.; Johnson, J. K. Molecular Simulations and Theoretical Predictions for Adsorption and Diffusion of CH4/H2 and CO2/CH4 Mixtures in ZIFs. *J. Phys. Chem. C* **2011**, *115* (25), 12560–12566.

(8)   Liu, Y.; Liu, J.; Chang, M.; Zheng, C. Effect of Functionalized Linker on CO2 Binding in Zeolitic Imidazolate Frameworks: Density Functional Theory Study. *J. Phys. Chem. C* **2012**, *116* (32), 16985–16991.

(9)   Han, S. S.; Kim, D.; Jung, D. H.; Cho, S.; Choi, S.-H.; Jung, Y. Accurate Ab Initio-Based Force Field for Predictive CO2 Uptake Simulations in MOFs and ZIFs: Development and Applications for MTV-MOFs. *J. Phys. Chem. C* **2012**, *116* (38), 20254–20261.

(10)   Salah, M.; Marakchi, K.; Dalbouha, S.; Senent, M. L.; Kabbaj, O. K.; Komiha, N. Influence of the Functionalization of Imidazole on Its CO2 Uptake Efficiency. A Theoretical Contribution. *Comput. Theor. Chem.* **2015**, *1073*, 1–8.

(11)   Boulmene, R.; Boussouf, K.; Prakash, M.; Komiha, N.; Al-Mogren, M. M.; Hochlaf, M. Ab Initio and DFT Studies on CO2 Interacting with Znq+–Imidazole (Q=0, 1, 2) Complexes: Prediction of Charge Transfer through σ- or π-Type Models. *ChemPhysChem* **2016**, *17* (7), 994–1005.

(12)   VandeVondele, J.; Krack, M.; Mohamed, F.; Parrinello, M.; Chassaing, T.; Hutter, J. Quickstep: Fast and Accurate Density Functional Calculations Using a Mixed Gaussian and Plane Waves Approach. *Comput. Phys. Commun.* **2005**, *167* (2), 103–128.

(13)   CP2K developers group, CP2K Code.http://www.cp2k.org .

(14)   Hohenberg, P.; Kohn, W. Inhomogeneous Electron Gas. *Phys. Rev.* **1964**, *136* (3B), B864–B871.

(15)   Kohn, W.; Sham, L. J. Self-Consistent Equations Including Exchange and Correlation Effects. *Phys. Rev.* **1965**, *140* (4A), A1133–A1138.

(16)   Lippert, B. G., Hutter, J., and Parrinrllo, M. A hybrid Gaussian and plane wave density functional scheme. Mol. Phys. 1997, 92, 477–488.

(17)   Perdew, J. P.; Chevary, J. A.; Vosko, S. H.; Jackson, K. A.; Pederson, M. R.; Singh, D. J.; Fiolhais, C. Atoms, Molecules, Solids, and Surfaces: Applications of the Generalized Gradient Approximation for Exchange and Correlation. *Phys. Rev. B* **1992**, *46* (11), 6671–6687.

(18)   Lehnert, R.; Seel, F. Darstellung Und Kristallstruktur Des Mangan(II)- Und Zink(II)-Derivates Des Imidazols. *Z. Für Anorg. Allg. Chem.* **1980**, *464* (1), 187–194.

(19)   Lewis, D. W.; Ruiz-Salvador, A. R.; Gómez, A.; Rodriguez-Albelo, L. M.; Coudert, F.-X.; Slater, B.; Cheetham, A. K.; Mellot-Draznieks, C. Zeolitic Imidazole Frameworks: Structural and Energetics Trends Compared with Their Zeolite Analogues. *CrystEngComm* **2009**, *11* (11), 2272–2276.

(20)   The Cambridge Crystallographic Data Centre, CCDC. www.ccdc.cam.ac.uk

(21)   Grimme, S., Antony, J., Ehrlich, S., & Krieg, H. A consistent and accurate ab initio parametrization of density functional dispersion correction (DFT-D) for the 94 elements H-Pu. J. Chem. Phys. 2010, 132, 154104.

(22)   VandeVondele, J., & Hutter, J. Gaussian basis sets for accurate calculations on molecular systems in gas and condensed phases. J. Chem. Phys. 2007,127, 114105.

(23)   Hartwigsen, C.; Goedecker, S.; Hutter, J. Relativistic Separable Dual-Space Gaussian Pseudopotentials from H to Rn. *Phys. Rev. B* **1998**, *58* (7), 3641–3662.

(24)   Goedecker, S.; Teter, M.; Hutter, J. Separable Dual-Space Gaussian Pseudopotentials. *Phys. Rev. B* **1996**, *54* (3), 1703–1710.

(25)   Krack, M. Pseudopotentials for H to Kr Optimized for Gradient-Corrected Exchange-Correlation Functionals. *Theor. Chem. Acc.* **2005**, *114* (1–3), 145–152.

(23)   VandeVondele, J., & Hutter, J. An efficient orbital transformation method for electronic structure calculations. J. Chem. Phys. 2003 ,118, 4365–4369.

(27) Khot, K. M.; Heer, P. K. K. S.; Biniwale, R. B.; Gaikar, V. G. Equilibrium Adsorption Studies of CO2, CH4, and N2 on Amine Functionalized Polystyrene. *Sep. Sci. Technol.* **2014**, *49* (15), 2376–2388.

(28) Mulliken, R. S. Electronic Population Analysis on LCAO–MO Molecular Wave Functions. I. *J. Chem. Phys.* **1955**, *23* (10), 1833–1840.

(29) Moghadam, P. Z.; Ivy, J. F.; Arvapally, R. K.; Santos, A. M. dos; Pearson, J. C.; Zhang, L.; Tylianakis, E.; Ghosh, P.; Oswald, I. W. H.; Kaipa, U.; et al. Adsorption and Molecular Siting of CO2, Water, and Other Gases in the Superhydrophobic, Flexible Pores of FMOF-1 from Experiment and Simulation. *Chem. Sci.* **2017**, *8* (5), 3989–4000.

TOC graphic

1
2
3
4
5
6
7
8